Journal of Renewable Materials

Tech Science Press

DOI: 10.32604/jrm.2023.024521

check for updates

ARTICLE

Fabricating Cationic Lignin Hydrogels for Dye Adsorption

Chao Wang, Xuezhen Feng, Wanbing Li, Shibin Shang* and Haibo Zhang*

Institute of Chemical Industry of Forest Products, CAF; National Engineering Laboratory for Biomass Chemical Utilization; Key Laboratory of Chemical Engineering of Forest Products, National Forestry and Grassland Administration; Key Laboratory of Biomass Energy and Material, Jiangsu Co-Innovation Center of Efficient Processing and Utilization of Forest Resources, Nanjing, 210042, China

*Corresponding Authors: Shibin Shang. Email: shangsb@163.com; Haibo Zhang. Email: shdzhanghaibo@163.com

Received: 01 June 2022 Accepted: 03 August 2022

ABSTRACT

Due to the low content of adsorption-active groups in lignin, its application in the field of adsorption is limited. Herein, we first prepared cationic kraft lignin acrylate, from which a cationic lignin (CKLA) hydrogel was further prepared by cationic kraft lignin acrylate, acrylamide, and N, N'-methylenebisacrylamide. The morphology, compression properties and swelling properties of CKLA hydrogels were investigated. The prepared CKLA hydrogel was applied as an adsorbent for Congo red. The effect of CKLA hydrogel dosages, initial concentration of Congo red, and pH on adsorption efficiency was investigated. The maximum Congo red removal efficiency was obtained at the initial concentration of Congo red of 50 mg/L, pH 7, and 5 mg dosage of CKLA hydrogel with 20% cationic lignin content. After five cycles of adsorption, the adsorption efficiency of the hydrogel for Congo red still reached more than 80%. The CKLA hydrogel showed pseudo-second-order adsorption kinetics for Congo red adsorption. These results demonstrate the potential of the CKLA hydrogel as an adsorbent for water treatment.

KEYWORDS

Adsorption; lignin; congo red; hydrogel

1 Introduction

With the discharge of a large amount of dye wastewater, the textile, printing and dyeing industries have caused serious water pollution [1,2]. Anion dyes are widely used in the dyeing process due to their simple synthetic process, low cost, and better staining performance [3,4]. During the process of anionic dyeing, the fabric needs to be washed several times to improve its dyeing fastness, resulting in the generation of a large amount of anionic dye wastewater [5], causing oxygen deficiency and jeopardizing the viability of aquatic animals and plants [6,7].

Several methods such as chemical methods (flocculation [8], advanced oxidation [9], etc.), biological methods (anaerobic, aerobic [10], etc.), membrane separation methods [11], and physical methods (adsorption, etc.) have been developed to treat dye wastewater. Adsorption [12] stands out among the above-mentioned methods because of its many advantages, e.g., low cost, easy operation, less secondary pollution, and good treatment effect. Hydrogels have a 3D cross-network structure, containing hydrophilic and reactive functional groups [13]. Classic superabsorbent hydrogels composed of polymerized acrylic acid and acrylamide are gradually being replaced due to being non-sustainable, non-biodegradable, and costly [14]. Compared to conventional adsorbents, biomass-based adsorption materials such as cellulose [15],

lignin [16], corn [17], and sugarcane [18] have the advantages of wide source, low price, easy availability, and biodegradability, providing the excellent prospect for developing environmentally friendly materials [16].

Many bio-based materials, including lignin, cellulose and chitosan, have been used as adsorbents [19,20]. However, cellulose and chitosan are expensive and difficult to modify due to poor solubility in solvents. Lignin is the second most abundant bioresource on our planet [21], which has phenylpropane nits with methoxyl, phenolic and aliphatic hydroxyl, and carboxyl groups [22,23]. Therefore, lignin has been used to prepare different value-added products, including functional hydrogels, due to its rich availability, renewable source, low cost, and unique physiochemical properties. Lignin hydrogels are significantly porous with a larger specific surface area and exhibit high mechanical strength and chemical stability [24,25].

Considering the fast-swelling properties and porous structure of lignin hydrogels, they can absorb dye molecules through chemical, electrostatic interactions and hydrogen bonding [26]. A based biosorbent hydrogel (AML) was prepared by grafting alkali lignin with methylamine and formaldehyde via Mannich reaction, which displayed with fast adsorption of Pb^{2+} and adsorption capacity of 60.5 mg/g [27]. Domínguez-Robles et al. Crosslinked lignin with a mixed solution of ammonium hydroxide, methyl vinyl ether, and maleic acid through ester bonds to obtain superabsorbent lignin hydrogels, showing good adsorption efficiency for methylene blue [28]. Noteworthy, lignin does not contain cationic groups and is only used as a crosslinking agent while preparing hydrogels.

In this work, a functional cationic lignin hydrogel (CKLA) has been prepared from the polymerization of cationic lignin acrylate, acrylamide and N, N'-methylenebisacrylamide, and the adsorption properties of the hydrogels for Congo red (Fig. 1) were investigated. The effect of the amount of lignin used for preparing hydrogel on the swelling rate of hydrogels was investigated. The optimized hydrogel was assessed at different time intervals for its adsorption under different pH and congo red initial concentrations. Furthermore, kinetics and isotherm studies were conducted to assess the viability of CKLA (biomasses cationic lignin hydrogel) as an adsorbent for the removal of congo red.

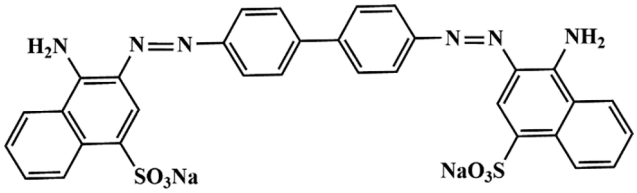

Figure 1: The chemical structure of congo red

2 Materials and Methods

2.1 Material

Kraft lignin was provided by Nanjing Shanhu Chemical Co., Ltd. (Nanjing, China). Glycidyl trimethyl ammonium chloride, N, N'-methylenebisacrylamide were obtained from Shanghai Macklin Biochemical Co., Ltd. (Shanghai, China). Acrylylchloride, acrylamide (AM), and Congo red were supplied by Aladdin Reagent (Shanghai) Co., Ltd. (Shanghai, China). Sodium bicarbonate was provided by Sinopharm Chemical Reagent Co., Ltd. (Shanghai, China). All the solvents and chemicals used in the syntheses and analyses were of analytical grade, obtained from commercial suppliers, and used without further purification.

2.2 Preparation of Cationic Lignin Acrylate

First, Kraft lignin (15 g), 2,3-epoxypropyl ammonium chloride (7.8 g) and benzyltrim-ethy-lammonium chloride (0.3 g) were dissolved in 30 g of N, N'-dimethylformamide, heated to 140°C and kept for 2 h, followed by cooling to room temperature. Next, $NaHCO_3$ (7.77 g) was added and mixed evenly. Acryloyl

chloride (8.38 g) was added dropwise to the above solution over 4 h. After the reaction, the mixture was poured into ethyl acetate for precipitation. Finally, the precipitate was vacuum-dried to obtain 19.70 g of cationic lignin acrylate.

2.3 Preparation of Cationic Lignin-Based Hydrogel

Different masses of cationic lignin acrylate, acrylamide and N, N'-methylenebis(2-propenamide) (MBA) were dissolved in water with respect to the V-50 catalyst, retaining the total mass of monomers be 10 wt%, under a nitrogen atmosphere for 15 min to remove oxygen. The mixture was reacted at 50°C for 4 h, affording the CK cationic lignin-based hydrogel (CKLA hydrogel).

2.4 Characterization

FTIR spectra were obtained using a spectrometer (Nicholas iS50, U.S.) in the scanning range of 4000–500 cm^{-1}. ^{31}P NMR spectra were recorded using a Bruker 500 MHz NMR spectrometer. UV-vis spectral investigations were carried out using a UV-vis spectrometer (UV-2450, Shimadzu). Elemental analysis was performed using an elemental analyzer (2400, PerkinElmer).

2.5 Adsorption Experiment of Congo red

Congo red aqueous solutions of various concentrations (10, 30, 50, 70, 100, and 150 mg/L) were prepared. The prescribed amount of CKLA hydrogels was added in 25 mL congo red aqueous solutions, and the resulting mixture was shaken for 24 h. Once the adsorption equilibrium was reached, the absorbance of the supernatant was measured by UV-vis spectroscopy, and the adsorption efficiency was calculated as follows:

$$\eta = \frac{C_0 - C_e}{C_0} \times 100\% \tag{1}$$

where C_0 and C_e are initial and equilibrated dye concentrations (mg/L), respectively.

The amount of adsorption was calculated as follows:

$$q_e = \frac{V \times (C_0 - C_e)}{m} \tag{2}$$

where C_0 and C_e are initial and equilibrated dye concentrations in the solution (mg/L), respectively; V is the volume (L) of the congo red solution, and M is the weight (g) of the adsorbent.

2.6 Adsorption Kinetics

The adsorption kinetics was studied to investigate can reveal the equilibrium state of the adsorption process and inspect the important parameters that provide the suitability of the CKLA hydrogel as an adsorbent. Therefore, during the adsorption kinetics experiment, the following optimal reaction conditions were used: the initial concentration of the CR solution was 50 mg/L, the pH was 7, and the dosage was 5 mg/25 mL for a time of 1000 min. The adsorption experiments were evaluated using the adsorption capacity, and the adsorption kinetic models were analyzed by the pseudo-first-order adsorption kinetic model, the pseudo-second-order adsorption kinetic model, the Webber-Morris intraparticle diffusion model, and the Elovich kinetic model.

3 Results and Discussion

3.1 Characterization of Kraft Lignin and Cationic Lignin-Based Acrylates

Various hydroxyl groups on lignin were studied by the 31P NMR spectrum. The various hydroxyl groups on lignin and their concentrations are shown in Fig. 2 and Table 1, respectively. They are aliphatic

OH, 5-substituted OH, guaiacyl OH, p-hydroxy OH, and carboxylic acid, and the peaks appearing were observed in 149.3–145.2, 144.4–140.2, 140.2–138.7, 138.7–136.6, 135.8–133.9 ppm, the corresponding contents were 2.42, 1.69, 1.89, 0.17, and 0.39 mmol/g, respectively.

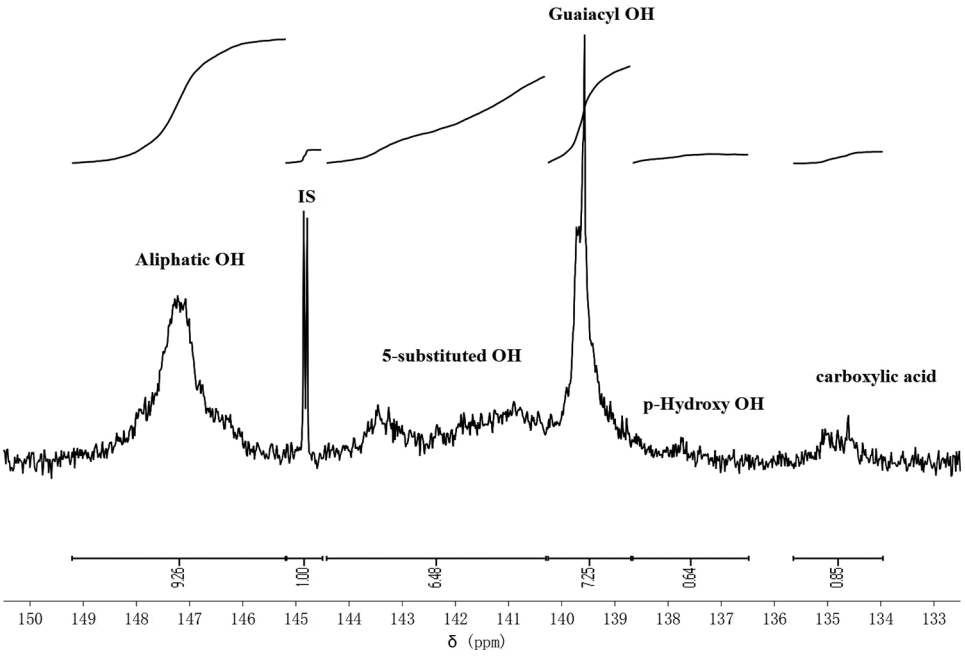

Figure 2: ^{31}P NMR spectrum of Kraft lignin

Table 1: Hydroxyl content in Kraft lignin (mmol/g)

Sample	Aliphatic OH	5-Substituted OH	Guaiacyl OH	p-Hydroxy OH	Carboxylic acid
Kraft lignin	2.42	1.69	1.89	0.17	0.39

The cationic lignin was obtained by reaction between the hydroxyl group in Kraft lignin and 2,3-epoxypropyl ammonium chloride, resulting in an epoxy ring-opening reaction to introduce a quaternary ammonium salt structure. Subsequently, the CKLA was prepared by the reaction of cationic lignin and acryloyl chloride (Fig. 4). The FTIR spectra of kraft lignin and CKLA are shown in Fig. 3. Compared with lignin, CKLA exhibited a noticeable decrease in the OH absorption peak at 3308 cm^{-1}. After the reaction of Kraft lignin with 2,3-epoxypropylammonium chloride and acryloyl chloride, an ester group peak at 1724 cm^{-1} and an unsaturated double bond peak at 1650 cm^{-1} appeared in the FT-IR spectra of CKLA. Furthermore, through elemental analysis (Table 2), the N content in kl was obtained to be 0, while it was 3.15% in CKLA, proving the successful synthesis of CKLA.

3.2 Preparation and Swelling Properties of CKLA Hydrogel

The preparation route of the cationic lignin-based hydrogel is delineated in Fig. 4. Concisely, CKLA hydrogels were prepared by copolymerization of cationic lignin-based acrylate, acrylamide, and N, N'-methylene bisacrylamide in an aqueous solution [29].

The swelling properties of CKLA hydrogels with different lignin content are shown in Fig. 5. The swelling ratio of all CKLA hydrogels increases gradually, then slowly reaches the swelling equilibrium. It is evident that the hydrogels reached the swelling equilibrium (the equilibrium swelling ratios of

hydrogels with different lignin contents are abbreviated as Seq-x, where x is the lignin content) after soaking in water for 13 h, and their trend was as follows: Seq-25 > Seq-20 > Seq-5 > Seq-15 > Seq-10 (Fig. 5). With the increased CKLA content, the quaternary ammonium salt group content also increased, resulting in higher equilibrium swelling ratios of hydrogels. However, Seq-5 is higher than Seq-15 and Seq-10; this is because the content of CKLA is low, leading to a low cross-link density [30].

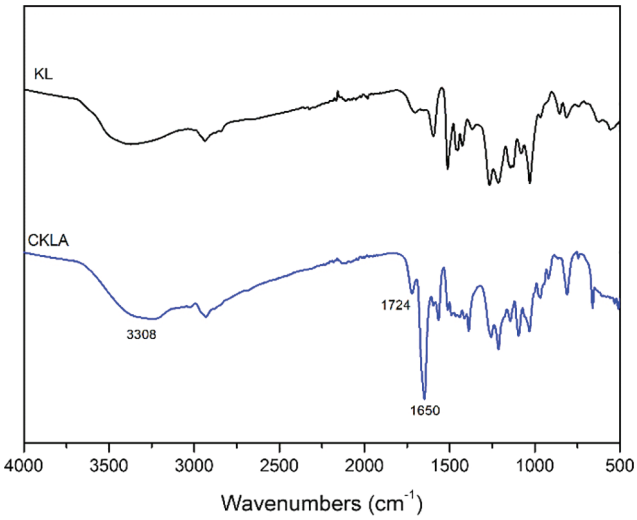

Figure 3: FT-IR spectra of Kraft lignin and CKLA

Table 2: Elemental analysis of Kraft lignin CKLA

	C	H	O	N
KL	61.74%	5.65%	28.97%	0
ACKL	57.77%	5.77%	22.92%	3.15%

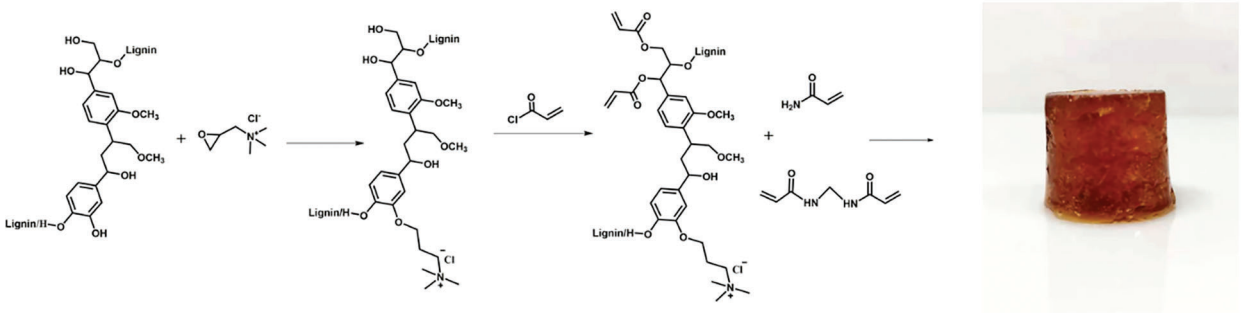

Figure 4: Synthetic route of CKLA hydrogels

3.3 Effect of the Dosage of CKLA Hydrogels on CR Adsorption

The effect of the dosage of various CKLA hydrogels on the adsorption of CR is shown in Fig. 6. The CR removal efficiency of hydrogels initially increased with the increasing amount of cationic lignin-based hydrogel and then reached the maximum. The adsorption efficiency obtained was the best for 20% lignin content, while the hydrogel dosage was 5 mg. The main reason affecting the adsorption is that with the

increase of the content of CKLA, the quaternary ammonium salt on the CKLA hydrogel also increases, which provides more adsorption sites and thus reduces the required dosage of CKLA hydrogels. A decrease in adsorption efficiency was observed for the CKLA hydrogel with 25% CKLA content due to the increase of quaternary ammonium content, which causes electrostatic repulsion [31].

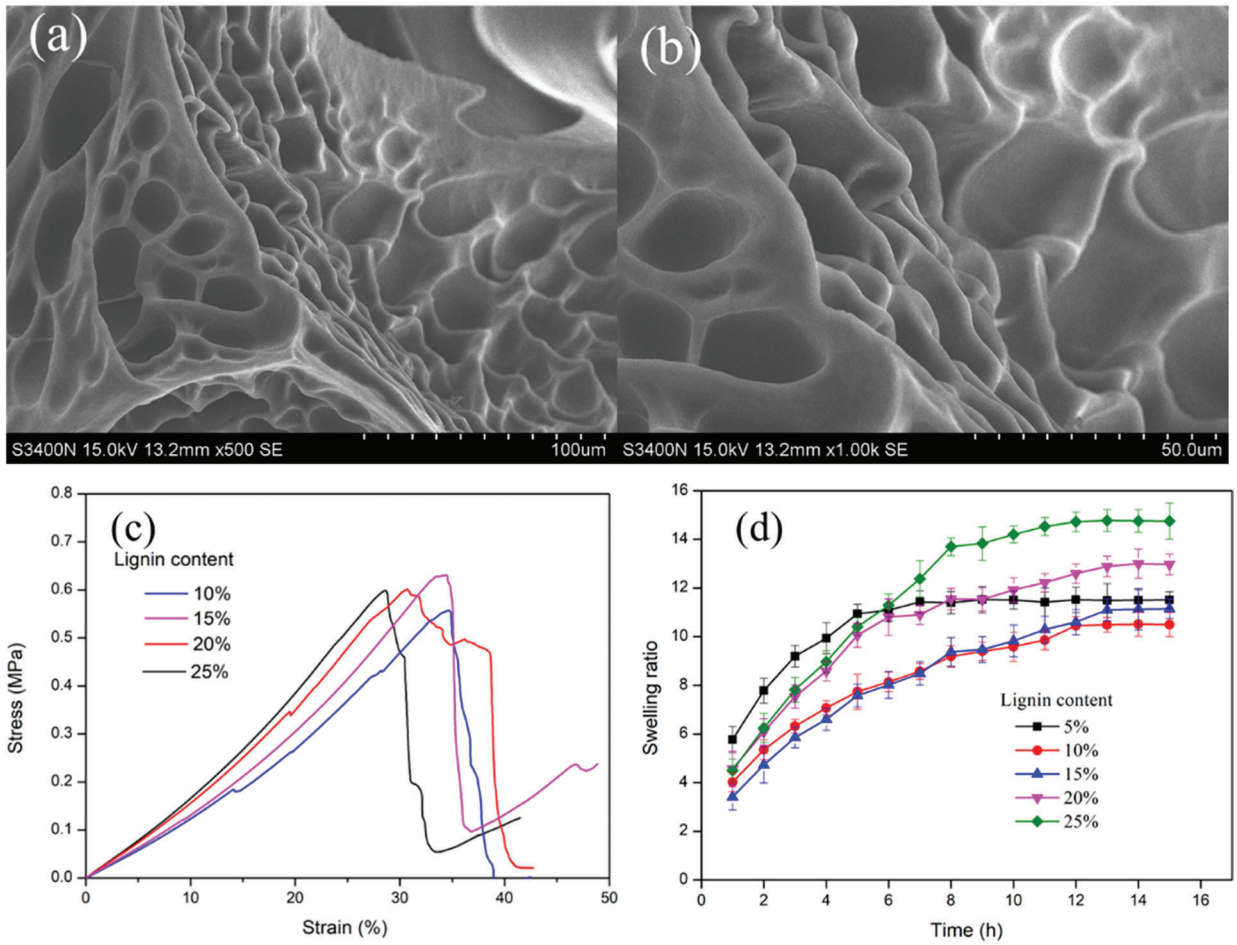

Figure 5: (a) and (b) The SEM images of CKLA hydrogel; (c) Compression stress-strain curves; (d) Swelling curves of CKLA hydrogels

3.4 Effect of CR Initial Concentration on Adsorption Efficiency

The effect of the initial concentration of Congo red on the removal efficiency of the prepared hydrogels is shown in Fig. 7. Upon increasing the concentration of Congo red solution progressively, the removal efficiency of cationic lignin-based hydrogel first showed an increasing trend. It reached the maximum for 50 mg/L Congo red aqueous solution, and further concentration increments resulted in the decline of the removal efficiency. A higher initial dye concentration will provide an enhanced propulsion force to accelerate the mass transfer resistance of dye molecules from the liquid phase to the solid phase (adsorbent), thereby improving the adsorption capacity of the hydrogel [32]. At the beginning of the adsorption process, there is a mass of vacancies on the surface of the adsorbent. The repulsive force between the Congo red molecules adsorbed on the surface of the adsorbent and present in the solution phase gradually weakens the effective adsorption sites of the adsorbent [33]. Thus the CKLA hydrogels

reach adsorption saturation at high Congo red concentrations, resulting in a decrease in the adsorption efficiency.

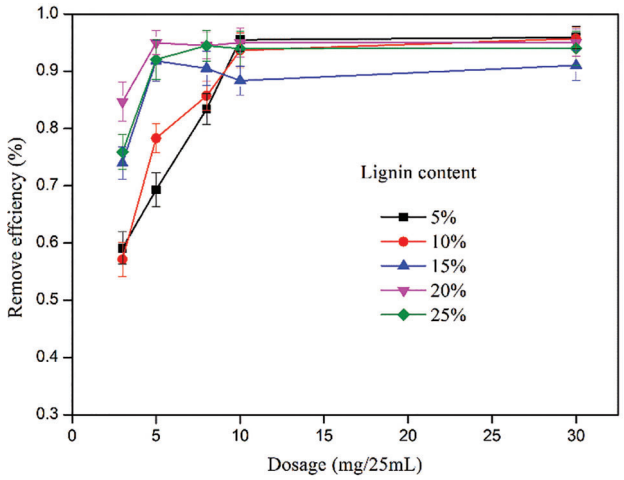

Figure 6: Effect of dosage of CKLA hydrogels on the adsorption of CR

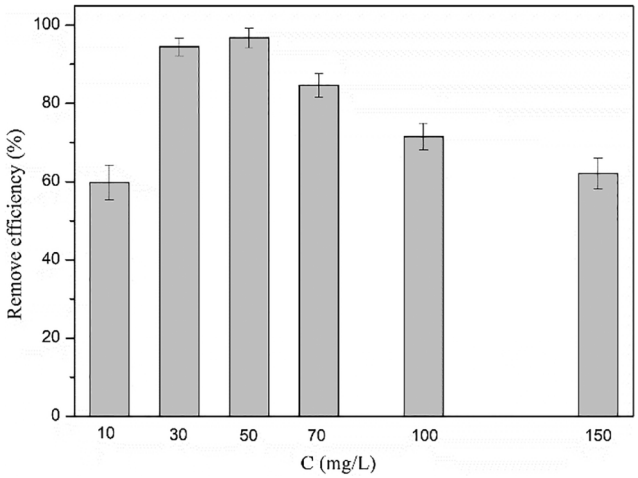

Figure 7: Effect of initial concentration of CR on removal efficiency of hydrogels

3.5 Effect of pH on Adsorption Efficiency

The effect of pH on the adsorption efficiency of cationic lignin-based hydrogels is shown in Fig. 8. It was observed that with the increase of pH value, the removal efficiency for Congo red by CKLA hydrogels first increased and then showed a decreasing trend. The maximum adsorption efficiency was obtained at pH 7. Under acidic conditions, the conversion of sodium sulfonate in Congo red to sulfonic acid groups weakens the electrostatic interaction with quaternary ammonium salt groups, resulting in low adsorption efficiency [34,35]. At pH > 7, the electrostatic repulsion between hydroxide ions and Congo red molecules [36], reduces removal efficiency.

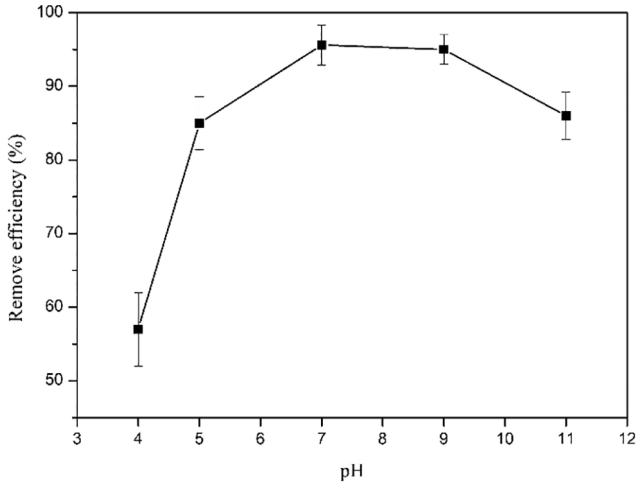

Figure 8: Effect of pH on the adsorption efficiency of CKLA hydrogels

3.6 Adsorption Kinetics

During the adsorption process, the diffusion of the adsorbate from the solution to the adsorbent and the rate at which the adsorbate accumulates on the surface of the adsorbent determine the kinetics of the adsorption process and the adsorption efficiency [37]. The adsorption time can indicate whether the whole adsorption process has reached an equilibrium state and evaluate the adsorption capacity of the adsorption process [38]. The effect of adsorption time on the adsorption of CR by CKLA hydrogels is illustrated in Fig. 9. Evidently, CKLA hydrogels reached adsorption equilibrium at 600 min.

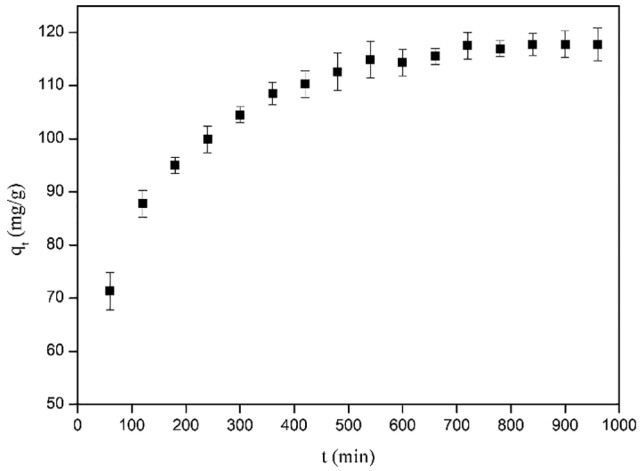

Figure 9: Effect of time on the adsorption efficiency of CKLA hydrogels

To describe the adsorption process more clearly, the adsorption kinetics of CR for CKLA hydrogel was investigated by various kinetic models: pseudo-first-order model: i.e., pseudo-second-order model, Webber-Morris Intral-particle diffusion model, and the Elovich model.

The pseudo-first-order model can be expressed by Eq. (3):

$$\ln(q_e - q_t) = \ln q_e - k_1 t \tag{3}$$

The pseudo-second-order model can be described by Eq. (4):

$$\frac{t}{q_t} = \frac{1}{k_2 q_e^2} + \frac{t}{q_e} \tag{4}$$

q_e is the amount of CR adsorbed at equilibrium (in mg/g), qt represents the CR adsorbed at time t (in mg/g), and k_1 and k_2 are the pseudo-first-order model and pseudo-second-order model constants, respectively.

The Webber-Morris Intral-particle diffusion model can be given by Eq. (5):

$$q_t = k_i t^{1/2} + C \tag{5}$$

The Elovich model can be given by Eq. (6):

$$q_t = \frac{1}{\beta}\ln(\alpha\beta) + \frac{1}{\beta}\ln t \tag{6}$$

where q_e and q_t are the same as previous. k_i is the rate constant for the Webber-Morris Intral-particle diffusion model, whereas α and β are the Elovich model rate constants.

Table 3 summarizes the three kinetic model fitting parameters and mass transfer process models for the adsorption of CR by CKLA. The linear fitting form of these models is displayed in Fig. 10. The pseudo-second-order kinetic model fitted the maximum adsorption capacity of 125.63 mg/g, close to the experimental value. Moreover, the pseudo-second-order kinetic model R2 had the best coefficient. Therefore, the adsorption process of CKLA hydrogel for Congo red was more consistent with the pseudo-second-order kinetic model, showing that the adsorption process is mainly chemical adsorption. Furthermore, the intra-particle diffusion model demonstrated that the adsorption process was the internal mass transfer.

Table 3: Kinetics parameters for CR adsorption by CKLA hydrogel

	Pseudo-first-order		Pseudo-second-order		Elovich model		Intra-particle diffusion model	
Parameter	q_e	k_1	q_e	k_2	α	β	k_i	C
value	69.14	$5.26 * 10^{-3}$	125.63	$1.21 * 10^{-4}$	17.11	0.057	2.1128	61.2766
r^2	0.9818		0.9868		0.9780		0.9228	

3.7 Reusability of CKLA Hydrogel

The reusability of CKLA hydrogel is shown in Fig. 11. The results showed that after five cycles of adsorption, the adsorption efficiency of the hydrogel for Congo red still reached more than 80%. This proved that the hydrogel had excellent reusability.

3.8 Possible Mechainism for the Adsorption of Congo Red by CKLA Hydrogel

The adsorption mechanisms tend to be electrostatic interactions between the quaternary ammonium group in the hydrogel and the sulfonate in Congo red [39]. Besides, Congo red is adsorbed through hydrogen bonding, van der Waals forces and hydrophobic interactions [40,41].

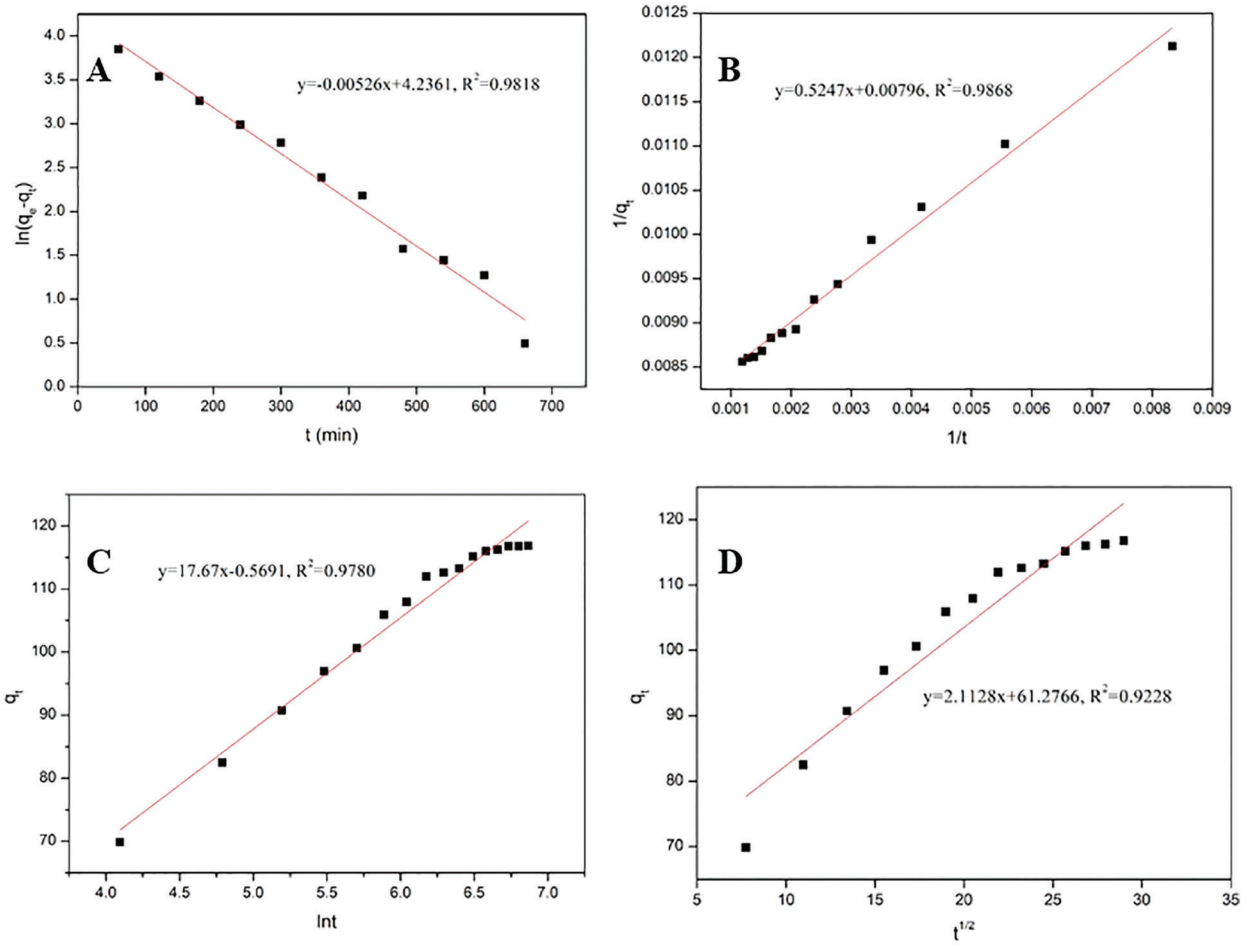

Figure 10: (A) Pseudo-first-order, (B) Pseudo-second-order, (C) Elovich model, and (D) Intra-particle diffusion models

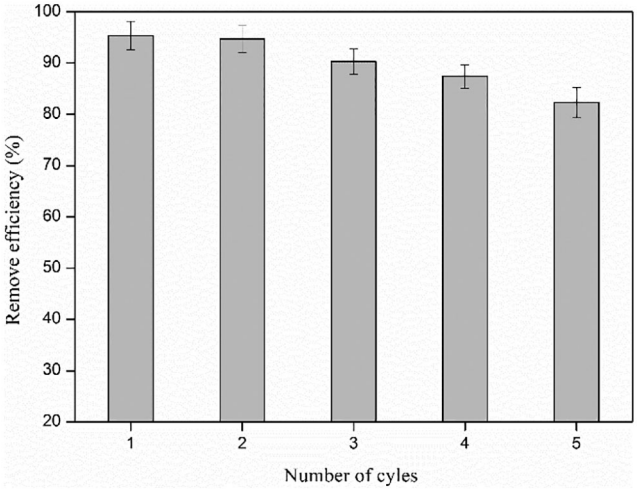

Figure 11: The reusability of CKLA hydrogel

4 Conclusion

In this work, cationic kraft lignin acrylate (CKLA) was prepared by reacting Kraft lignin with 2,3-epoxypropyl ammonium chloride and acryloyl chloride. Cationic lignin hydrogels were further synthesized by polymerization of acrylamide, MBA, and CKLA. The effect of dosage of CKLA hydrogels, initial concentration of Congo red, and pH on the adsorption efficiency of the prepared hydrogels was investigated. The optimum Congo red removal efficiency was obtained for the hydrogel with 20% lignin content, 5 mg hydrogel dosage, 50 mg/L concentration of Congo red aqueous solution, and pH = 7. Adsorption kinetics studies revealed that the adsorption of CR by CKLA hydrogels followed pseudo-second-order kinetics.

Funding Statement: This study was supported by Fundamental Research Funds of CAF (CAFYBB2020MB002).

Conflicts of Interest: The authors declare that they have no conflicts of interest to report regarding the present study.

References

1. Kant, R. (2012). Textile dyeing industry an environmental hazard. *Natural Science, 4,* 22–26. DOI 10.4236/ns.2012.41004.
2. Zhang, C. G., Chen, H., Xue, G., Liu, Y. B., Chen, S. P. et al. (2021). A critical review of the aniline transformation fate in azo dye wastewater treatment. *Journal of Cleaner Production, 321,* 128971. DOI 10.1016/j.jclepro.2021.128971.
3. Zheng, J. L., Du, L. L., Gao, P., Chen, K. W., Ma, L. L. et al. (2021). Mino-modified biomass for highly efficient removal of anionic dyes from aqueous solutions. *Journal of the Taiwan Institute of Chemical Engineers, 119,* 136–145. DOI 10.1016/j.jtice.2021.01.026.
4. Alsantali, R. I., Raja, Q. A., Alzahrani, A. Y. A., Sadiq, A., Naeem, N. et al. (2022). Miscellaneous azo dyes: A comprehensive review on recent advancements in biological and industrial applications. *Dyes and Pigments, 199,* 110050. DOI 10.1016/j.dyepig.2021.110050.
5. Karaman, C., Karaman, O., Show, P. L., Karimi-Maleh, H., Zare, N. (2022). Congo red dye removal from aqueous environment by cationic surfactant modified-biomass derived carbon: Equilibrium, kinetic, and thermodynamic modeling, and forecasting via artificial neural network approach. *Chemosphere, 290,* 133346. DOI 10.1016/j.chemosphere.2021.133346.
6. Hassan, M., Carr, M. C. (2020). Biomass-derived porous carbonaceous materials and their composites as adsorbents for cationic and anionic dyes: A review. *Chemosphere, 265,* 129087. DOI 10.1016/j.chemosphere.2020.129087.
7. Han, Q., Yang, Y., Wang, R., Zhang, K., Liu, N. et al. (2021). Biochar derived from agricultural wastes as a means of facilitating the degradation of Azo dyes by sulfides. *Catalysts, 11,* 434. DOI 10.3390/catal11040434.
8. Sun, Y., Li, D., Lu, X., Sheng, J., Zheng, X. et al. (2021). Flocculation of combined contaminants of dye and heavy metal by nano-chitosan flocculants. *Journal of Environmental Management, 299,* 113589. DOI 10.1016/j.jenvman.2021.113589.
9. Ismail, G. A., Sakai, H. (2022). Review on effect of different type of dyes on advanced oxidation processes (AOPs) for textile color removal. *Chemosphere, 291,* 132906. DOI 10.1016/j.chemosphere.2021.132906.
10. Rathi, B. S., Kumar, P. S. (2022). Sustainable approach on the biodegradation of azo dyes: A short review. *Current Opinion in Green and Sustainable Chemistry, 33,* 100578. DOI 10.1016/j.cogsc.2021.100578.
11. Chen, Y., Sun, R., Yan, W., Wu, M., Zhou, Y. et al. (2022). Antibacterial polyvinyl alcohol nanofiltration membrane incorporated with $Cu(OH)_2$ nanowires for dye/salt wastewater treatment. *Science of the Total Environment, 817,* 152897. DOI 10.1016/j.scitotenv.2021.152897.
12. Gao, L., Gao, T., Zhang, Y., Hu, T. (2021). A bifunctional 3D porous Zn-MOF: Fluorescence recognition of Fe^{3+} and adsorption of Congo red/methyl orange dyes in aqueous medium. *Dyes and Pigments, 119,* 109945.
13. Shen, B., Guo, Z., Huang, B., Zhang, G., Fei, P. et al. (2022). Preparation of hydrogels based on pectin with different esterification degrees and evaluation of their structure and adsorption properties. *International Journal of Biological Macromolecules, 202,* 397–406. DOI 10.1016/j.ijbiomac.2021.12.160.

14. Bello, K., Sarojini, B. K., Narayana, B., Rao, A., Byrappa, K. (2018). A study on adsorption behavior of newly synthesized banana pseudo-stem derived superabsorbent hydrogels for cationic and anionic dye removal from effluents. *Carbohydrate Polymers, 181,* 605–615. DOI 10.1016/j.carbpol.2017.11.106.
15. Zhong, L., He, F., Liu, Z., Dong, B., Ding, J. (2022). Adsorption of uranium (VI) ions from aqueous solution by acrylic and diaminomaleonitrile modified cellulose. *Colloids and Surfaces A: Physicochemical and Engineering Aspects, 641,* 128565. DOI 10.1016/j.colsurfa.2022.128565.
16. Chen, H., Liu, T., Meng, Y., Cheng, Y., Lu, J. et al. (2020). Novel graphene oxide/aminated lignin aerogels for enhanced adsorption of malachite green in wastewater. *Colloids and Surfaces A: Physicochemical and Engineering Aspects, 603,* 125281. DOI 10.1016/j.colsurfa.2020.125281.
17. Wang, F., Li, L., Iqbal, J., Yang, Z., Du, Y. (2022). Preparation of magnetic chitosan corn straw biochar and its application in adsorption of amaranth dye in aqueous solution. *International Journal of Biological Macromolecules, 199,* 234–242. DOI 10.1016/j.ijbiomac.2021.12.195.
18. Tahir, H., Sultan, M., Akhtar, N., Hameed, U., Abid, T. (2016). Application of natural and modified sugar cane bagasse for the removal of dye from aqueous solution. *Journal of Saudi Chemical Society, 20(S1),* S115–S121. DOI 10.1016/j.jscs.2012.09.007.
19. Cheng, Z., Li, J., Wang, B., Zeng, J., Chen, K. (2020). Scalable and robust bacterial cellulose carbon aerogels as reusable absorbents for high-efficiency oil/water separation. *ACS Applied Bio Materials, 3(11),* 7483–7491. DOI 10.1021/acsabm.0c00708.
20. Zhu, S., Xu, J., Kuang, Y., Cheng, Z., Wu, Q. et al. (2021). Lignin-derived sulfonated porous carbon from cornstalk for efficient and selective removal of cationic dyes. *Industrial Crops and Products, 159,* 113071. DOI 10.1016/j.indcrop.2020.113071.
21. Vedula, S. S., Yadav, G. D. (2022). Wastewater treatment containing methylene blue dye as pollutant using adsorption by chitosan lignin membrane: Development of membrane, characterization and kinetics of adsorption. *Journal of the Indian Chemical Society, 99(1),* 100263. DOI 10.1016/j.jics.2021.100263.
22. Mondal, A. K., Xu, D., Wu, S., Zou, Q., Huang, F. et al. (2022). Design of Fe^{3+} -rich, high-conductivity lignin hydrogels for supercapacitor and sensor applications. *Biomacromolecules, 23(3),* 766–778. DOI 10.1021/acs.biomac.1c01194.
23. Heo, J. W., An, L., Chen, J., Bae, J. H., Kim, Y. S. (2022). Preparation of amine-functionalized lignins for the selective adsorption of Methylene blue and Congo red. *Chemosphere, 295,* 133815. DOI 10.1016/j.chemosphere.2022.133815.
24. Alsamhary, K., Al-Enazi, N. M., Alhomaidi, E., Alwakeel, S. (2022). Spirulina platensis mediated biosynthesis of Cuo Nps and photocatalytic degradation of toxic azo dye Congo red and kinetic studies. *Environmental Research, 207,* 112172. DOI 10.1016/j.envres.2021.112172.
25. An, L., Si, C., Bae, J. H., Jeong, H., Kim, Y. S. (2020). One-step silanization and amination of lignin and its adsorption of Congo red and Cu(II) ions in aqueous solution. *International Journal of Biological Macromolecules, 159,* 222–230. DOI 10.1016/j.ijbiomac.2020.05.072.
26. Barus, D. A., Humaidi, S., Ginting, R. T., Sitepu, J. (2020). Enhanced adsorption performance of chitosan/cellulose nanofiber isolated from durian peel waste/graphene oxide nanocomposite hydrogels. *Environmental Nanotechnology, Monitoring & Management, 17,* 100650. DOI 10.1016/j.enmm.2022.100650.
27. Ge, Y., Song, Q., Li, Z. (2015). A mannich base biosorbent derived from alkaline lignin for lead removal from aqueous solution. *Journal of Industrial & Engineering Chemistry, 23,* 228–234. DOI 10.1016/j.jiec.2014.08.021.
28. Domínguez-Robles, J., Peresin, M. S., Tamminen, T., Rodríguez, A., Larrañeta, E. et al. (2018). Lignin-based hydrogels with "super-swelling" capacities for dye removal. *International Journal of Biological Macromolecules, 115,* 1249–1259. DOI 10.1016/j.ijbiomac.2018.04.044.
29. Zhang, J., Peppas, N. A. (2002). Morphology of poly(methacrylic acid)/poly(n-isopropyl acrylamide) interpenetrating polymeric networks. *Journal of Biomaterials Science Polymer Edition, 13(5),* 511–525. DOI 10.1163/15685620260178373.
30. Ban, M. T., Mahadin, N., Karim, K. J. A. (2022). Synthesis of hydrogel from sugarcane bagasse extracted cellulose for swelling properties study. *Materials Today Proceedings, 50(6),* 2567–2575. DOI 10.1016/j.matpr.2021.08.342.

31. Xia, M., Gao, R., Xu, G., You, Y., Li, X. et al. (2022). Fabrication and investigation of novel monochloroacetic acid fortified, tripolyphosphate-crosslinked chitosan for highly efficient adsorption of uranyl ions from radioactive effluents. *Journal of Hazardous Materials, 431,* 128461. DOI 10.1016/j.jhazmat.2022.128461.
32. Dai, H., Huang, Y., Zhang, H., Ma, L., Huang, H. et al. (2020). Direct fabrication of hierarchically processed pineapple peel hydrogels for efficient Congo red adsorption. *Carbohydrate Polymers, 230,* 115599. DOI 10.1016/j.carbpol.2019.115599.
33. Qin, Q., Li, M., Lan, P., Liao, Y., Sun, S. et al. (2021). Novel $CaCO_3$/chitin aerogel: Synthesis and adsorption performance toward Congo red in aqueous solutions. *International Journal of Biological Macromolecules, 181,* 786–792. DOI 10.1016/j.ijbiomac.2021.03.116.
34. Li, P., Wang, T., He, J., Jiang, J., Lei, F. (2021). Synthesis, characterization, and selective dye adsorption by pH- and ion-sensitive polyelectrolyte galactomannan-based hydrogels. *Carbohydrate Polymers, 264,* 118009. DOI 10.1016/j.carbpol.2021.118009.
35. Chowdhury, A., Kumari, S., Khan, A. A., Hussain, S. (2021). Synthesis of mixed phase crystalline $CoNi_2S_4$ nanomaterial and selective mechanism for adsorption of Congo red from aqueous solution. *Journal of Environmental Chemical Engineering, 9(6),* 106554. DOI 10.1016/j.jece.2021.106554.
36. Tang, J., Zhang, Y. F., Liu, Y., Li, Y., Hu, H. (2020). Efficient ion-enhanced adsorption of congo red on polyacrolein from aqueous solution: Experiments, characterization and mechanism studies. *Separation and Purification Technology, 252,* 117445. DOI 10.1016/j.seppur.2020.117445.
37. Zhou, D., Brusseau, M. L., Zhang, Y., Li, S., Wei, W. et al. (2021). Simulating PFAS adsorption kinetics, adsorption isotherms, and nonideal transport in saturated soil with tempered one-sided stable density (TOSD) based models. *Journal of Hazardous Materials, 411(2),* 125169. DOI 10.1016/j.jhazmat.2021.125169.
38. Xiong, Y., Woodward, R. T., Danaci, D., Evans, A., Tian, T. et al. (2021). Understanding trade-offs in adsorption capacity, selectivity and kinetics for propylene/propane separation using composites of activated carbon and hypercrosslinked polymer. *Chemical Engineering Journal, 426,* 131628. DOI 10.1016/j.cej.2021.131628.
39. Pandey, S., Do, J. Y., Kim, J., Kang, M. (2020). Fast and highly efficient removal of dye from aqueous solution using natural locust bean gum based hydrogels as adsorbent. *International Journal of Biological Macromolecules, 143,* 60–75. DOI 10.1016/j.ijbiomac.2019.12.002.
40. Shen, C., Shen, Y., Wen, Y., Wang, H., Liu, W. (2011). Fast and highly efficient removal of dyes under alkaline conditions using magnetic chitosan-Fe(III) hydrogel. *Water Research, 45(16),* 5200–5210. DOI 10.1016/j.watres.2011.07.018.
41. Hu, X., Liang, R., Sun, G. (2018). Super-adsorbent hydrogel for removal of methylene blue dye from aqueous solution. *Journal of Materials Chemistry, A, 6(36),* 17612–17624. DOI 10.1039/C8TA04722G.